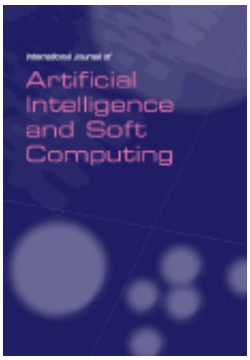

International Journal of Artificial Intelligence and Soft Computing

ISSN online: 1755-4969 - ISSN print: 1755-4950
https://www.inderscience.com/ijaisc

Rotor fault characterisation in induction motors under different load levels via machine learning methods

Hayri Arabacı, Mücahid Barstuğan

DOI: 10.1504/IJAISC.2024.10064252

Article History:

Received:	06 April 2023
Last revised:	23 January 2024
Accepted:	19 February 2024
Published online:	04 July 2024

Rotor fault characterisation in induction motors under different load levels via machine learning methods

Hayri Arabacı

Department of Electrical and Electronics Engineering,
Faculty of Technology,
Selcuk University,
Konya, Türkiye
Email: hayriarabaci@selcuk.edu.tr

Mücahid Barstuğan*

Department of Electrical and Electronics Engineering,
Faculty of Engineering and Natural Sciences,
Konya Technical University,
Konya, Türkiye
Email: mbarstugan@ktun.edu.tr

Abstract: Induction motors stand out for their robustness and are widely used in the industrial sector. Literature studies have focused more on rotor faults because rotor fault signatures are hard to detect. In most experimental studies, tests were carried out using a single motor for fault classification. In general, training and fault classification was conducted on a single load type. This study focused on fault classification for induction motors with varying powers and load conditions. Motor current data for four different induction motors and randomly selected load levels were obtained, a classifier structure was formed using machine learning, and tests were carried out. Classification results for the five classifiers were obtained and compared to determine the reliability of the generalised classifier structure. Support vector machines and k-nearest neighbour methods were used in the classification and k-nearest neighbour achieved at 99.51% accuracy.

Keywords: fault classification; induction motor; machine learning; pattern recognition; rotor faults.

Reference to this paper should be made as follows: Arabacı, H. and Barstuğan, M. (2024) 'Rotor fault characterisation in induction motors under different load levels via machine learning methods', *Int. J. Artificial Intelligence and Soft Computing*, Vol. 8, No. 2, pp.129–146.

Biographical notes: Hayri Arabacı completed his Master study on 'Electric motor malfunctions' in 2006. In his Doctoral study, he examined 'The effects of malfunctions on engine performance' and completed it in 2010. He has been working as a Professor Doctor position in Electrical and Electronics Engineering Department at Technology Faculty in Selcuk University since 2019.

Mücahid Barstuğan graduated from Electronics and Communication Engineering Department of Kocaeli University with BSc degree in 2010 from Electrical and Electronics Engineering Department of Selcuk University with MSc degree in 2014, and from Electrical and Electronics Engineering Department of Konya Technical University with PhD degree in 2019. He is working at Electrical and Electronics Engineering Department of Konya Technical University as a researcher. His profession includes ensemble learning, industrial image analysis, artificial intelligence, object detection, and pattern recognition.

1 Introduction

Induction motors are well-known for their robustness and are widely used in the industrial sector for their affordability. Any fault in the motor affects its efficiency and performance and so the system it drives, which negatively affects connected production processes. Therefore, induction motor faults have been examined by numerous researchers for many years. Induction motor faults are evaluated under four different groups (Hassan et al., 2018):

- stator faults
- rotor faults
- misalignment faults
- roller faults.

Stator faults are easy to detect with simple methods. Other faults are not as easily detected and require in-depth analysis (Vas, 1993). These three fault types are generally detected by vibration analysis, sound analysis, and current analysis methods (Hassan et al., 2018). To obtain the vibration signals for vibration analysis, vibration sensors need to be connected to the motor and the system to which it is connected (Nath et al., 2020; Morales-Perez et al., 2018). Sensors are difficult to place, require precision, and are expensive. Therefore, the usage of vibration analysis to detect motor faults is on the decline. For sound analysis, microphones and ultrasonic sensors are used for fault detection with sound signals (Yaman, 2021). However, it is difficult to distinguish between sound information which carries fault data from background noise since motors are generally found in noisy environments. This complicates fault detection with sound analysis. Also, there are rotor fault detection studies that use FEM-based motor magnetic flux measurement (Panagiotou et al., 2019a, 2019b). However, FEM-based implementations require a high processing load.

In the current analysis method, motor current data obtained from just one current sensor can be utilised for fault detection. Moreover, current sensors are inexpensive, and connecting them to the system is easy. For this reason, recent literature studies have focused on fault detection with current analysis (Hassan et al., 2018).

Initial fault detection studies focused primarily on revealing the fault feature. Subsequent studies, however, aimed to determine whether the motor was defective or intact (Haji and Toliyat, 2001). In recent years, the focus of such studies has been on fault classification in addition to fault detection. Time and frequency domains are used for the

extraction of rotor fault features. The time domain is not commonly used in fault classification because it has large amounts of data and the effects of rotor bar fault on the current signal are insignificant. The frequency-domain for feature extraction yields better results since the effects of rotor bar fault occur in multiples of the base current frequency component due to slip as shown in equation (1). Thus, fault detection studies have focused more on the frequency domain. In equation (1), s is slip value; f is fundamental current frequency.

$$f_{brb} = (1 \pm 2ks) f \tag{1}$$

Studies using time-frequency domains together are also being conducted (Panagiotou et al., 2019b; Romero-Troncoso et al., 2016). The use of only the frequency domain for feature extraction has increased since the fault effects are more pronounced, the number of features is low and therefore the processing load is reduced. Numerous methods have been used to obtain rotor bar fault frequency components: discrete wavelet transform (Antonino-Daviu et al., 2006; Ordaz-Moreno et al., 2008; Sadeghian et al., 2009; Siddiqui and Giri, 2012), Prony analysis (Chen and Živanović, 2010), fast Fourier transform (FFT) (Didier et al., 2007; Ameid et al., 2017a, 2017b), zoom-FFT (Kim et al., 2012), Hilbert transform (Bessam et al., 2015; Rangel-Magdaleno et al., 2017), extended Kaman filter (Naha et al., 2016), multiple signal classification (Singh and Naikan, 2018), autoregressive model (Ayhan et al., 2008). Equation (1) shows that rotor bar fault effects have close values to the fundamental current component. Therefore, it is sufficient to examine frequency components close to the fundamental current component (sidebands). FFT is used to zoom into this frequency interval for feature extraction; thus, a feature matrix with less data is obtained.

In recent years, deep learning (Paul et al., 2023; Sakallı and Koyuncu, 2023) has witnessed notable advancements, with the development of sophisticated neural network architectures addressing various challenges in computer vision and beyond. Residual networks (Das et al., 2022c) introduced a breakthrough architectural innovation by incorporating skip connections or residual blocks. This design mitigates the vanishing gradient problem, allowing for the training of extremely deep networks (Sahu et al., 2023) with hundreds or even thousands of layers. MobileNetV2 (Das and Meher, 2021), on the other hand, focuses on efficient convolutional operations, making it well-suited for mobile and edge devices. It utilises inverted residuals and linear bottlenecks to achieve a good balance between model size and accuracy. These developments collectively represent a trend towards more efficient, scalable, and powerful deep learning models, enabling advancements in tasks such as image classification, object detection, and semantic segmentation. Researchers continue to explore novel architectures, optimisation techniques, and transfer learning strategies to push the boundaries of deep learning capabilities across various domains.

Rotor faults are usually caused by manufacturing errors. However, not all errors are at the same level- some faults cause the rotor bar to lose its conductivity entirely (a broken rotor bar fault) whereas some faults cause a significant reduction in conductivity (high reactance bar fault). When a motor is first used after its production, existing faults have the potential to develop further as the bars are exposed to magnetic and thermal stress. A high-reactance bar fault can turn into a broken rotor bar fault. One broken rotor bar can cause a second broken rotor bar to form. For this reason, the following fault situations were included in the fault detection studies:

- no-fault
- high-reactance
- one broken bar
- two broken bars
- three broken bars
- broken end-ring.

The worsening of rotor fault with motor operation makes it crucial for faults to be detected in the initial stages. For this reason, correct fault classification is essential. Some classifier methods such as adaptive neural fuzzy inference system (Sadeghian et al., 2009; Mohamed et al., 2021), artificial neural network (ANN) (Zolfaghari et al., 2017; Bessam et al., 2016), principal component analysis (Georgoulas et al., 2013), support vector machines (SVM) (Thakur et al., 2021; Arabaci and Mohamed, 2020; Keskes et al., 2013), k-nearest neighbourhood (k-NN) (Yaman, 2021), and random forests (Quiroz et al., 2018) are used to classify rotor bar faults. In recent years, literature works have focused more on SVM and k-NN classifier techniques (Nath et al., 2021). These classification studies generally used only one motor. A classification set is created by taking motor current values usually only for no-load or full-load values from one motor. By using one of these data values, accurate classification results were obtained. However, two questions arise here:

1 Can the classifier structure, which is trained on one motor, classify another motor that has different nominal power?

2 With the classification structure obtained, can it give the same accuracy for a different load than the load case used in the tests?

This study used four different motors with different power ratings to answer these questions. Each motor was operated on different levels of loads. Current values for each motor were obtained for five fault conditions and no-fault conditions. A separate classifier structure was created for each motor. Besides, a classifier structure (generalised classifier), which was trained on all motors, was created. The obtained results were compared for the five different classifier structures. The results showed that the generalised classifier had high classification accuracy even if the motor power and load level were changed. The literature studies mostly limited with one motor power and load level. Also, the data in this study was acquired on motors operating in the factory. So, the data has other environmental effects on the motor signals. In addition, this study combined all data from different motors and load levels and proposes one classifier structure to detect different types of stator faults.

This study has four sections. The second section explains the signals and dataset used. The third and fourth sections present the experimental setup and classification results, respectively. The fifth section concludes the findings obtained.

2 Material and method

2.1 Material

In a healthy motor, rotor currents flow evenly through the rotor bars. If the current passing through one of the bars decreases or does not flow at all, the magnetic flux in the air gap is adversely affected. These effects are reflected on the current drawn by the motor as frequency components [equation (1)] depending on the slip and fundamental frequency of the motor current. These frequency components, referred to as sidebands, can be found to the right or left side of the base principal component. In the frequency spectrum of the motor current, rotor bar fault effects can be sought by looking at these components. The location of these components in the spectrum and the amplitude of these components vary according to the magnitude of the rotor bar fault and the loading state of the motor. For this reason, even if motor rotor faults can be detected by simply looking at the sidebands, it is difficult to determine the magnitude (class) of the fault.

This study aimed to classify rotor faults regardless of motor power and the motor load condition. For this purpose, four different induction motors were loaded at various load levels and current values were obtained. The frequency spectrum from the current data was obtained using FFT. Differences in motor power and load conditions cause rotor faults to affect the spectrum in different ways. To evaluate similar fault conditions under the same motor conditions, the frequency spectrum was normalised. The frequency interval of 28–72 Hz, where fault indications are most intense on the spectrum, was used as input data for the classifier structure. The frequency spectrum obtained, and the frequency region used for the feature matrix is given in Figure 1.

Figure 1 The frequency spectrum of motor current and the frequency area used as features (see online version for colours)

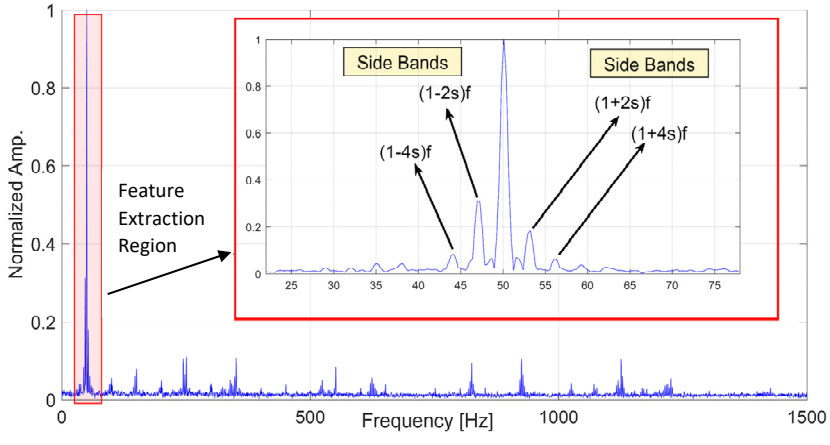

This study examined six different rotor faults. Each motor current was obtained under three different load levels for all different fault conditions. Each dataset was created by sampling the current signal for three seconds. One signal vector has 20,000 points for one motor condition. Three different datasets were prepared from the signals. Figure 2 presents the dataset preparation process.

Figure 2 The dataset preparation process (see online version for colours)

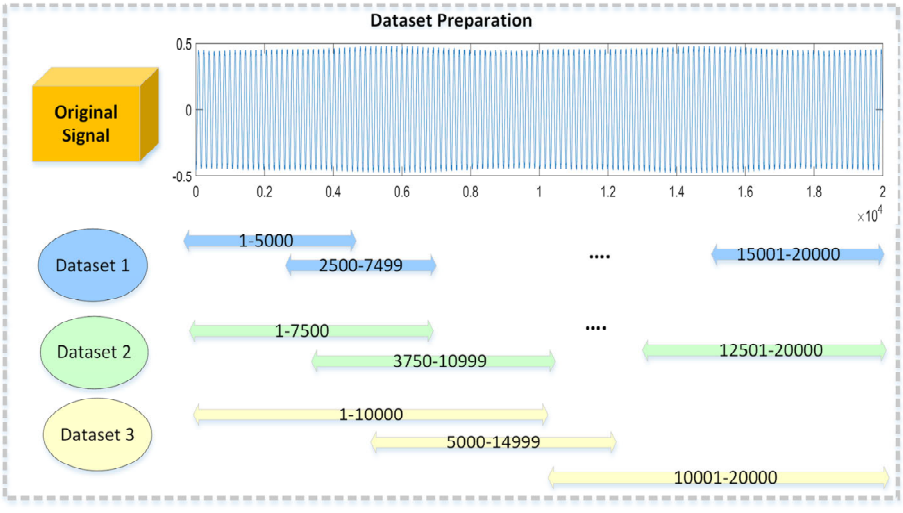

The aim of preparing three different datasets is to increase the number of samples for each motor. Also, this process gives information about if the classification performance increases when the number of samples increases. Table 1 presents the number of samples for three datasets of all motor types.

Table 1 The number of samples for three datasets of all motor types

Motor type	*Fault types*	*Dataset 1*	*Dataset 2*	*Dataset 3*
Motor 1	No-fault	450	360	270
	High reactance	480	384	288
	One broken bar	450	360	270
	Two broken bars	450	360	270
	Three broken bars	360	288	216
	Broken end-ring	540	432	324
Motor 2	No fault	270	216	162
	High reactance	255	204	153
	One broken bar	255	204	153
	Two broken bars	270	216	162
	Three broken bars	270	216	162
	Broken end-ring	275	220	165
Motor 3	No fault	360	288	216
	High reactance	360	288	216
	One broken bar	360	288	216
	Two broken bars	360	288	216
	Three broken bars	375	300	225
	Broken end-ring	360	288	216

Table 1 The number of samples for three datasets of all motor types (continued)

Motor type	*Fault types*	*Dataset 1*	*Dataset 2*	*Dataset 3*
Motor 4	No fault	270	216	162
	High reactance	270	216	162
	One broken bar	270	216	162
	Two broken bars	285	228	171
	Three broken bars	270	216	162
	Broken end-ring	270	216	162
Motors 1, 2, 3 and 4	No fault	1,350	1,080	810
	High reactance	1,365	1,092	819
	One broken bar	1,335	1,068	801
	Two broken bars	1,365	1,092	819
	Three broken bars	1,275	1,020	765
	Broken end-ring	1,445	1,156	867

FFT method was applied to the raw signals in Table 1. The FFT signal that is between 28–72 Hz interval has 150 data points. Figure 3 shows the signals for different rotor fault classes for dataset 1.

Figure 3 FFT results for different rotor fault types (see online version for colours)

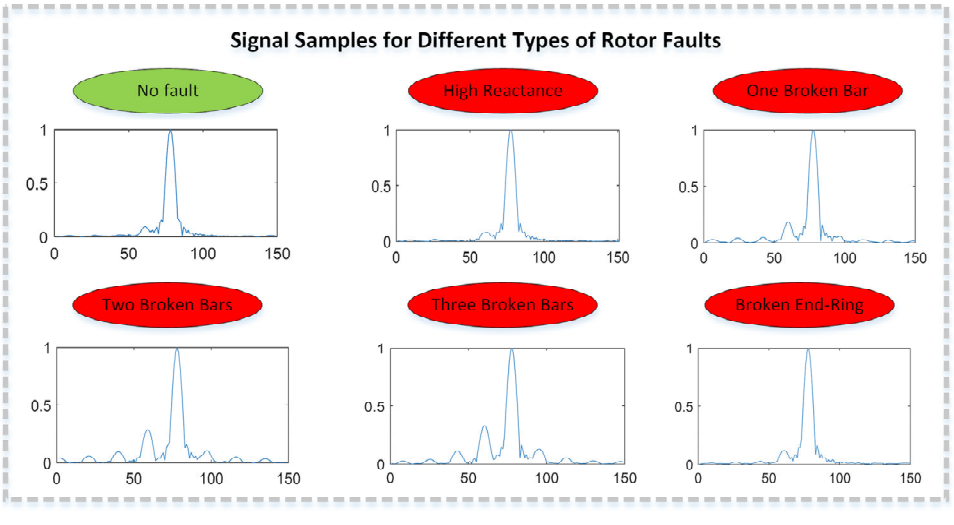

2.2 Method

This study used k-NN and SVM methods as classifiers. In the classification stage, the three datasets created from motors 1, 2, 3 and 4, respectively – were classified separately. Figure 4 shows the preparation of datasets 1, 2 and 3 on a sample signal that belongs to motor 1.

Figure 4 Two broken bars sample signal from motor 1 (see online version for colours)

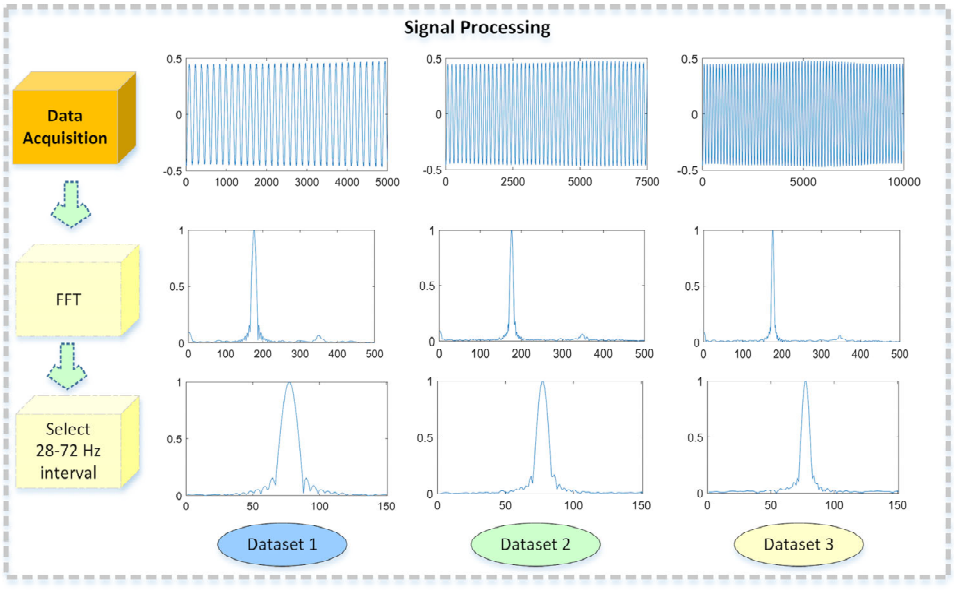

Figure 4 shows that the same signal has different shapes for three different datasets. This study examined if this situation affects classification performance. After classifying the four different motor datasets, all datasets were combined, and one dataset was prepared. The new combined dataset was also classified by k-NN and SVM methods; thus, the performance of the rotor fault classifier was evaluated regardless of motor nominal power and load level for different types of induction motors. Figure 5 presents the training process used in this study.

Figure 5 The proposed rotor faults classifier method (see online version for colours)

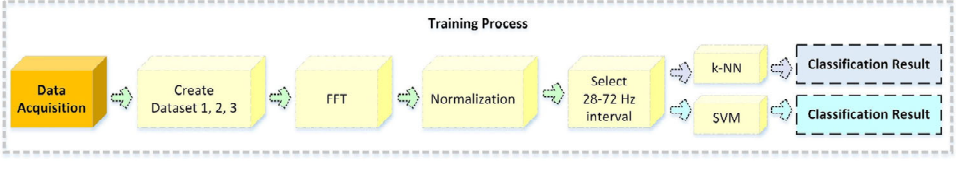

2.3 Machine learning

Machine learning is a subfield of artificial intelligence that empowers computer systems to learn and improve from experience without explicit programming. It involves the development of algorithms and models that enable computers to analyse and interpret data, identify patterns, and make decisions or predictions. The process often begins with feeding the machine learning model large sets of data, allowing it to recognise underlying patterns and relationships. As the model learns and iterates, it becomes more adept at making accurate predictions or classifications on new, unseen data. Machine learning finds applications in various domains, from image and speech recognition to recommendation systems, making it a pivotal technology in the advancement of

intelligent systems (Das et al., 2022a). SVM, k-NN, ANN, deep learning, AdaBoost are some of machine learning methods.

2.3.1 Support vector machines

SVMs are a powerful class of supervised machine learning algorithms designed for classification and regression tasks. The fundamental principle behind SVM is to find the optimal hyperplane that separates different classes in a high-dimensional space. This hyperplane is chosen in such a way that it maximises the margin, which is the distance between the hyperplane and the nearest data points of each class. SVM excels in handling both linear and nonlinear relationships in data using kernel functions that map input data into higher-dimensional spaces. SVMs are known for their ability to handle complex decision boundaries and perform well in scenarios with limited data. They have found applications in various fields, including image classification (Nurrani et al., 2023), text categorisation (Bamgboye et al., 2023), and biomedical imaging (Das et al., 2019, 2022b), making them a versatile tool in the machine learning toolkit.

2.3.2 k-nearest neighbours)

k-NN is a simple yet effective machine learning algorithm used for classification and regression tasks. The core idea of k-NN is to classify a data point based on the majority class of its k-NNs in the feature space. The 'k' in k-NN represents the number of neighbours considered for the classification, and it is a crucial parameter that influences the algorithm's performance. In the case of classification, the algorithm assigns the class label that is most prevalent among the k neighbours, while in regression, it predicts the average or weighted average of the target values. K-NN is a non-parametric, instance-based learning method, making it particularly useful for scenarios with complex and nonlinear relationships. However, its performance can be sensitive to the choice of distance metric and the value of k, and it may not scale well with large datasets. Despite these considerations, k-NN remains a versatile and intuitive algorithm, often used for its simplicity and effectiveness in various applications such as medical image segmentation (Das et al., 2021), motor health control systems (Kumar and Upadhyaya, 2023).

3 Experimental study

This experimental study used a motor-generator experiment setup. A generator was connected to the motor shaft to load the motors. The motors were loaded under different levels by a resistive load that was connected to the generator terminals. The block diagram of the experimental setup is given in Figure 6.

Figure 6 Experimental setup block diagram

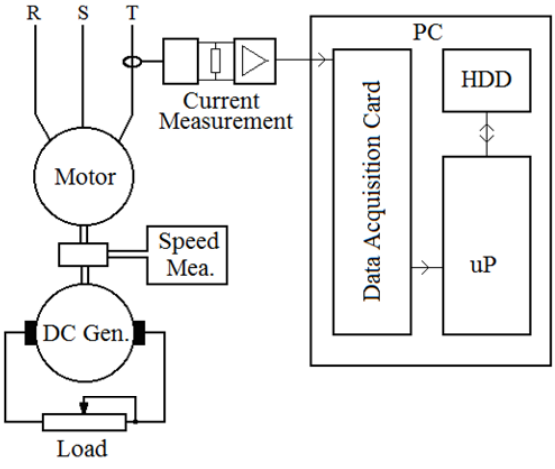

Four different motors with powers of 50HP, 30HP, 25HP, and 10HP were used in the experiments. All motors were 3-phase, with a 380V nominal voltage and 50Hz frequency. Six different conditions (six classes) were examined for each of the motors:

- no-fault
- high-reactance
- one broken bar
- two broken bars
- three broken bars
- broken end-ring.

Each of the fault conditions was created in a factory environment. First, to obtain a high-reactance rotor bar fault, one of the rotor bars was drilled 5 mm deep with a drill bit smaller than the bar diameter. Doing so caused the electron transition surface to become smaller; thus, the bar resistance was increased. To create a broken rotor bar, instead of driving the copper rotor bar through the rotor, it was hammered in 2 parts, one on the left and one on the right, leaving a 10mm gap in the axial direction. By doing so, the electron transfer was eliminated. This same process was applied to create two and three rotor bar faults. For the end-ring fault, the ring was split in a lathe to lose its conductivity in the axial direction. Photographs of the defective rotors created and three of the motors used are shown in Figure 7. After creating the faults, the rotors were balanced and mounted to prevent a negative effect on the current due to unbalance, thus avoiding possible confusion with rotor bar faults.

Figure 7 The rotor bar faults, (a) high-reactance fault (b) broken end-ring fault (c) broken bar faults (d) the motors used (see online version for colours)

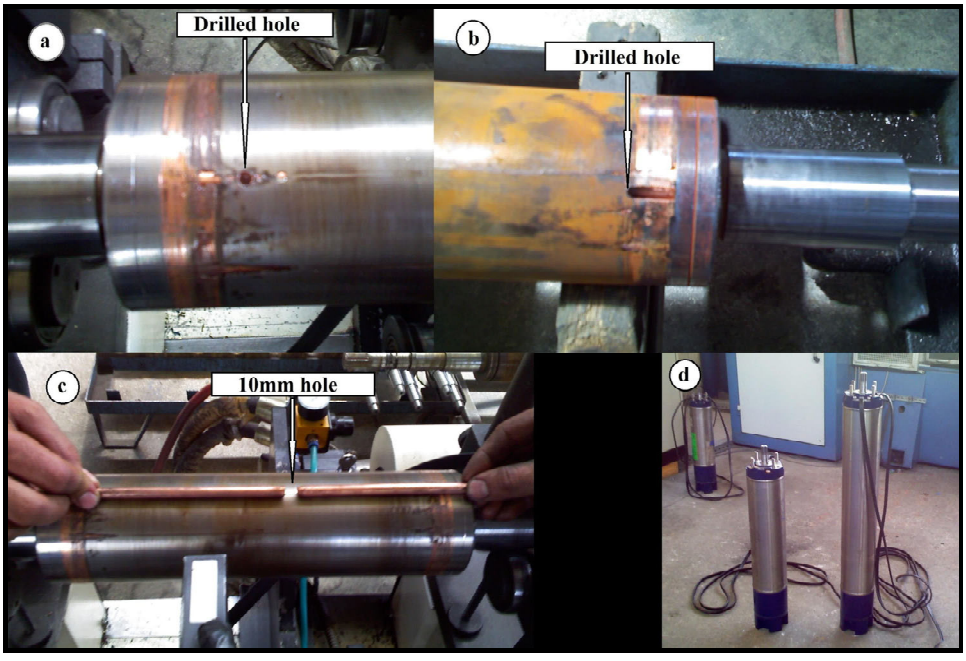

In experimental studies, the motor current was obtained from only one phase. LA-205-S Hall-effect current sensor of LEM company was used to read the current. Advantech PCI-1716 data card was used to obtain current sensor data. The sampling frequency was set at 7,500 Hz. The data was saved to the computer. The photograph of the experimental setup (test unit) from which the data was taken is shown in Figure 8.

Figure 8 Experimental test unit (see online version for colours)

To extract features from each data, the current data in the time domain was transformed to the frequency domain using FFT. The frequency region between 28 and 72 Hz, where the indications are most noticeable, was taken as input data for the classification. Experimental results were obtained by using this input data in the training and testing of the classification structure.

4 Experimental results

This section consists of two parts. The first part presents the results of each motor, separately. The second part presents the classification results of all motors. Sensitivity (Sen), specificity (Spe), accuracy (Acc), and G-mean metrics were used to examine the classification results. 2-fold, 5-fold, and 10-fold cross-validation methods were used during the training process. SVM and k-NN techniques were applied to classify all datasets.

4.1 Single motor analyses

In this section, the classification results of the motors 1, 2, 3 and 4 datasets have been analysed. The classification results were obtained using a confusion matrix. The classification process was applied to datasets 1, 2 and 3 of four different induction motors. 2-fold, 5-fold, and 10-fold cross-validation methods were used during the classification. Table 2 presents the best classification results of k-NN and SVM classifiers.

Table 2 The classification results for each motor

Motor	*Dataset*	*Classifier*	*k-fold*	*Sen (mean ± std)*	*Spe (mean ± std)*	*Acc (mean ± std)*	*G-mean (mean ± std)*
Motor 1	Dataset 3	k-NN	10	99.69 ± 0.6	99.88 ± 0.2	*99.83 ± 0.3*	99.79 ± 0.4
	Dataset 3	SVM	10	88.82 ± 1.7	95.52 ± 0.8	93.6 ± 1.1	92.11 ± 1.3
Motor 2	Dataset 2	k-NN	10	99.69 ± 0.5	99.87 ± 0.2	*99.82 ± 0.3*	99.78 ± 0.4
	Dataset 3	SVM	10	98.43 ± 1.4	99.37 ± 0.6	99.1 ± 1.4	98.9 ± 1
Motor 3	Dataset 2	k-NN	10	99.66 ± 0.5	99.86 ± 0.2	*99.8 ± 0.3*	99.76 ± 0.1
	Dataset 3	SVM	5	97.4 ± 1.4	98.97 ± 0.6	98.53 ± 0.8	98.18 ± 0.9
Motor 4	Dataset 3	k-NN	10	100	100	*100*	100
	Dataset 3	SVM	5	97.45 ± 1.3	98.96 ± 0.5	98.52 ± 0.8	98.2 ± 0.9

As Table 2 indicates, the best classification performance for all motor types was achieved with the k-NN classifier. The classification accuracies for motors 1, 2, 3 and 4 were obtained as 99.83%, 99.82%, 99.8%, and 100%, respectively. While the best classification performance was obtained with dataset 3 in motors 1 and 4, it was obtained with dataset 2 in motors 2 and 3. The highest classification accuracy was always achieved in all trials with 10-fold cross-validation. SVM method reached the highest classification accuracy in motor 2 with dataset 3 as 99.1%.

4.2 Collective motor analysis

In this section, motors 1, 2, 3 and 4 datasets were combined and collective classification results were obtained for three separate datasets. The methods applied in the single motor analysis were also applied in the collective motor analysis.

Table 3 Classification results for each of the combined datasets

Motor	*Dataset*	*Classifier*	*k-fold*	*Sen (mean ± std)*	*Spe (mean ± std)*	*Acc (mean ± std)*	*G-mean (mean ± std)*
Motors 1, 2, 3 and 4	Dataset 1	k-NN	10	98.07 ± 0.6	99.23 ± 0.3	98.9 ± 0.4	98.65 ± 0.4
	Dataset 1	SVM	10	78.25 ± 1.6	91.15 ± 0.7	87.42 ± 0.9	84.45 ± 1.2
Motors 1, 2, 3 and 4	Dataset 2	k-NN	10	98.02 ± 0.9	99.21 ± 0.4	98.87 ± 0.6	98.61 ± 0.7
	Dataset 2	SVM	10	80.27 ± 1.4	91.76 ± 0.6	88.38 ± 0.9	85.82 ± 1.1
Motors 1, 2, 3 and 4	Dataset 3	k-NN	10	99.14 ± 0.6	99.66 ± 0.2	*99.51 ± 0.3*	99.4 ± 0.4
	Dataset 3	SVM	5	81.05 ± 1.5	92.21 ± 0.6	88.96 ± 0.8	86.45 ± 1.1

As indicated in Table 3, the k-NN method achieved the best classification accuracy on dataset 3 with 99.51% performance. SVM method classified dataset 3 with 88.96% accuracy. The k-NN method obtained more than 10% higher classification performance than the SVM method on all datasets. The proposed method classified signals from six different conditions of the four different induction motors each with high classification accuracy. The confusion matrix of the highest classification results is presented in Table 4.

Table 4 The confusion matrix for the proposed method (see online version for colours)

		No-fault	*One broken bar*	*Two broken bars*	*Three broken bars*	*Broken end-ring*	*High reactance*
Actual	No-fault	798	0	1	0	4	7
	One broken bar	0	800	0	0	0	1
	Two broken bars	2	0	817	0	0	0
	Three broken bars	2	0	0	763	0	0
	Broken end-ring	0	1	1	0	862	3
	High reactance	17	1	1	0	1	799
		Predicted					

As can be seen in Table 4, 17 ‘high reactance’ class signals were classified as ‘no-fault’ classes. Similarly, seven ‘no-fault’ class signals were detected as ‘high reactance’ class signals. ‘Three broken bars’ results show only two signals were detected as ‘no-fault’ class signals, while no other type of signal was found to have a ‘three broken bars’ signal. This indicates that ‘three broken bars’ signals can be detected with higher accuracy than other class signals. The optimum classifier structure obtained as a result of the experiments is presented in Figure 9.

Figure 9 The test process scheme (see online version for colours)

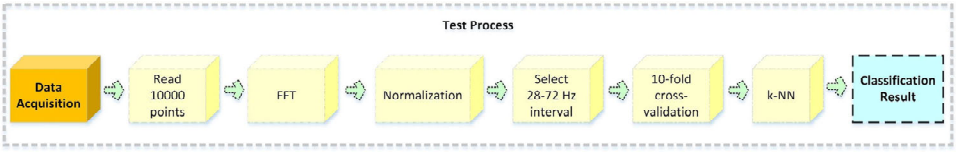

5 Discussion

This study implemented the detection and classification of rotor faults of induction motors. Rotor fault indicators are not obvious; thus, an in-depth analysis of the motor current is required. For this purpose, the motor current was obtained and transformed to the frequency domain using FFT. Fault-induced frequency components in the frequency domain were detected and used as input data for classification. This study formed two different classifier structures for both singular and multiple motor analysis and the results were compared.

The detection and diagnosis of rotor faults are still being studied in the literature. Table 5 presents recent rotor fault classification studies.

Table 5 Recent rotor fault classification studies

Study	*Year*	*Method*	*Motor types*	*Data*	*Fault types*	*Accuracy (%)*
Palácios et al. (2020)	2020	RBF-ANN	2	Current	3	90
Devarajan et al. (2021)	2020	ANFIS	1	Thermal camera images	4	91.27
Gao et al. (2021)	2021	LSTM	1	---	9	98.33
Marmouch et al. (2021)	2021	PCA-RBFNN	1	Current	4	98.42
Rodrigues et al. (2022)	2022	PCA-SVM	1	Vibration	5	79.4
Patil et al. (2022)	2022	SVM	1	Vibration	2	88.9
This study	2024	SVM	1	Current	6	99.1
This study	2024	k-NN	1	Current	6	100
This study	2024	SVM	4	Current	6	88.96
This study	*2024*	*k-NN*	*4*	*Current*	*6*	*99.51*

When literature studies regarding rotor faults were examined, it was seen that studies were mostly conducted on a single type of motor. This study analysed four different motors and three different load levels and achieved high classification performance. The results for both singular and collective motor analysis show that the proposed method can be used for rotor fault classification. Table 5 shows that the literature studies used k-NN and SVM methods for rotor fault classification and achieved satisfying results. This study indicates that:

- The longer the sampling data, the more accurate the classification process can be. Current signal data of different lengths (5,000, 7,500, and 10,000 samples) were used

in the classifier training and testing phases. Test results showed that the current signal which had 10,000 samples gave more accurate results.

- Both classifier methods achieved high classification accuracy.
- The classifier structure for four motor types can be used for different rated powers.
- A reliable classifier structure for rotor fault detection can be created via machine learning methods.
- Machine learning-based test setup can be used in the motor robustness determination after production.

In the literature studies, the approach of transforming motor signals into spectrogram images and subsequent feature extraction from these images has proven to be a promising methodology for motor fault classification. Therefore, we will use the signal data and transform them into spectrogram images. Also, by using image augmentation methods, the number of images will be increased, and so deep learning methods will be implemented on the data. As the field progresses, ongoing research efforts in refining image-based approaches to motor fault classification are crucial for advancing the accuracy and reliability of fault diagnosis systems in real-world industrial applications.

References

Ameid, T., Menacer, A., Talhaoui, H. and Harzelli, I. (2017a) 'Broken rotor bar fault diagnosis using fast Fourier transform applied to field-oriented control induction machine: simulation and experimental study', *The International Journal of Advanced Manufacturing Technology*, Vol. 92, pp.917–928, https://doi.org/10.1007/s00170-017-0143-2.

Ameid, T., Menacer, A., Talhaoui, H. and Harzelli, I. (2017b) 'Rotor resistance estimation using extended Kalman filter and spectral analysis for rotor bar fault diagnosis of sensorless vector control induction motor', *Measurement*, Vol. 111, pp.243–259, https://doi.org/10.1016/j.measurement.2017.07.039.

Antonino-Daviu, J., Riera-Guasp, M., Roger-Folch, J., Martínez-Giménez, F. and Peris, A. (2006) 'Application and optimization of the discrete wavelet transform for the detection of broken rotor bars in induction machines', *Applied and Computational Harmonic Analysis*, Vol. 21, No. 2, pp.268–279, https://doi.org/10.1016/j.acha.2005.12.003.

Arabaci, H. and Mohamed, M. (2020) 'A knowledge-based diagnosis algorithm for broken rotor bar fault classification using FFT, principal component analysis and support vector machines', *International Journal of Intelligent Engineering Informatics*, Vol. 8, No. 1, pp.19–37, https://doi.org/10.1504/IJIEI.2020.105431.

Ayhan, B., Trussell, H.J., Chow, M.Y. and Song, M.H. (2008) 'On the use of a lower sampling rate for broken rotor bar detection with DTFT and AR-based spectrum methods', *IEEE Transactions on Industrial Electronics*, Vol. 55, No. 3, pp.1421–1434, https://doi.org/10.1109/TIE.2007.896522.

Bamgboye, P.O., Adebiyi, M.O., Adebiyi, A.A., Osang, F.B., Adebiyi, A.A., Enwere, M.N. and Shekari, A. (2023) 'Text classification on customer review dataset using support vector machine', *Intelligent Sustainable Systems: Selected Papers of WorldS4*, Vol. 2, pp.407–415, https://doi.org/10.1007/978-981-19-7663-6_38.

Bessam, B., Menacer, A., Boumehraz, M. and Cherif, H. (2015) 'DWT and Hilbert transform for broken rotor bar fault diagnosis in induction machine at low load', *Energy Procedia*, Vol. 74, pp.1248–1257, https://doi.org/10.1016/j.egypro.2015.07.769.

Bessam, B., Menacer, A., Boumehraz, M. and Cherif, H. (2016) 'Detection of broken rotor bar faults in induction motor at low load using neural network', *ISA Transactions*, Vol. 64, pp.241–246, https://doi.org/10.1016/j.isatra.2016.06.004.

Chen, S. and Živanović, R.J.M. (2010) 'Estimation of frequency components in stator current for the detection of broken rotor bars in induction machines', *Measurement*, Vol. 43, No. 7, pp.887–900, https://doi.org/10.1016/j.measurement.2010.03.006.

Das, P.K. and Meher, S. (2021) 'An efficient deep convolutional neural network based detection and classification of acute lymphoblastic leukemia', *Expert Systems with Applications*, Vol. 183, p.115311, https://doi.org/10.1016/j.eswa.2021.115311.

Das, P.K., Diya, V., Meher, S., Panda, R. and Abraham, A. (2022a) 'A systematic review on recent advancements in deep and machine learning based detection and classification of acute lymphoblastic leukemia', *IEEE Access*, Vol. 10, pp.81741–81763, https://doi.org/10.1109/ACCESS.2022.3196037.

Das, P.K., Meher, S., Panda, R. and Abraham, A. (2019) 'A review of automated methods for the detection of sickle cell disease', *IEEE Reviews in Biomedical Engineering*, Vol. 13, pp.309–324, https://doi.org/10.1109/RBME.2019.2917780.

Das, P.K., Meher, S., Panda, R. and Abraham, A. (2021) 'An efficient blood-cell segmentation for the detection of hematological disorders', *IEEE Transactions on Cybernetics*, Vol. 52, No. 10, pp.10615–10626, https://doi.org/10.1109/TCYB.2021.3062152.

Das, P.K., Nayak, B. and Meher, S. (2022b) 'A lightweight deep learning system for automatic detection of blood cancer', *Measurement*, Vol. 191, p.110762, https://doi.org/10.1016/j.measurement.2022.110762.

Das, P.K., Sahoo, B. and Meher, S. (2022c) 'An efficient detection and classification of acute leukemia using transfer learning and orthogonal softmax layer-based model', *IEEE/ACM Transactions on Computational Biology and Bioinformatics*, Vol. 20, No. 3, pp.1817–1828, https://doi.org/10.1109/TCBB.2022.3218590.

Devarajan, G., Chinnusamy, M. and Kaliappan, L. (2021) 'Detection and classification of mechanical faults of three phase induction motor via pixels analysis of thermal image and adaptive neuro-fuzzy inference system', *Journal of Ambient Intelligence and Humanized Computing*, Vol. 12, pp.4619–4630, https://doi.org/10.1007/s12652-020-01857-8.

Didier, G., Ternisien, E., Caspary, O. and Razik, H. (2007) 'A new approach to detect broken rotor bars in induction machines by current spectrum analysis', *Mechanical Systems and Signal Processing*, Vol. 21, No. 2, pp.1127–1142, https://doi.org/10.1016/j.ymssp.2006.03.002.

Gao, Y., Liu, X., Huang, H. and Xiang, J. (2021) 'A hybrid of FEM simulations and generative adversarial networks to classify faults in rotor-bearing systems', *ISA transactions*, Vol. 108, pp.356–366, https://doi.org/10.1016/j.isatra.2020.08.012.

Georgoulas, G., Mustafa, M.O., Tsoumas, I.P., Antonino-Daviu, J.A., Climente-Alarcon, V., Stylious, C.D. and Nikolakopoulos, G. (2013) 'Principal component analysis of the start-up transient and hidden Markov modeling for broken rotor bar fault diagnosis in asynchronous machines', *Expert Systems with Applications*, Vol. 40, No. 17, pp.7024–7033, https://doi.org/10.1016/j.eswa.2013.06.006.

Haji, M. and Toliyat, H. (2001) 'Pattern recognition-a technique for induction machines rotor broken bar detection', *IEEE Transactions on Energy Conversion*, Vol. 16, No. 4, pp.312–317, https://doi.org/10.1109/60.969469.

Hassan, O.E., Amer, M., Abdelsalam, A.K. and Williams, B.W. (2018) 'Induction motor broken rotor bar fault detection techniques based on fault signature analysis – a review', *IET Electric Power Application*, Vol. 12, No. 7, pp.895–907, https://doi.org/10.1049/iet-epa.2018.0054.

Keskes, H., Braham, A. and Lachiri, Z. (2013) 'Broken rotor bar diagnosis in induction machines through stationary wavelet packet transform and multiclass wavelet SVM', *Electric Power Systems Research*, Vol. 97, pp.151–157, https://doi.org/10.1016/j.epsr.2012.12.013.

Kim, Y.H., Youn, Y.W., Hwang, D.H., Sun, J.H. and Kang, D. (2012) 'High-resolution parameter estimation method to identify broken rotor bar faults in induction motors', *IEEE Transactions on Industrial Electronics*, Vol. 60, No. 9, pp.4103–4117, https://doi.org/10.1109/TIE.2012.2227912.

Kumar, H. and Upadhyaya, G. (2023) 'Fault diagnosis of rolling element bearing using continuous wavelet transform and K-nearest neighbour', *Materials Today: Proceeding*, Vol. 92, No. 1, pp.56–60, https://doi.org/10.1016/j.matpr.2023.03.618.

Marmouch, S., Aroui, T. and Koubaa, Y. (2021) 'Statistical neural networks for induction machine fault diagnosis and features processing based on principal component analysis', *IEEJ Transactions on Electrical and Electronic Engineering*, Vol. 16, No. 2, pp.307–314, https://doi.org/10.1002/tee.23298.

Mohamed, M.A., Mohamed, A.A.A., Abdel-Nasser, M., Mohamed, E.E. and Hassan, M.A.M. (2021) 'Induction motor broken rotor bar faults diagnosis using ANFIS-based DWT', *International Journal of Modelling and Simulation*, Vol. 41, No. 3, pp.220–233, https://doi.org/10.1080/02286203.2019.1708173.

Morales-Perez, C., Rangel-Magdaleno, J., Peregrina-Barreto, H., Amezquita-Sanchez, J.P. and Valtierra-Rodriguez, M. (2018) 'Incipient broken rotor bar detection in induction motors using vibration signals and the orthogonal matching pursuit algorithm', *IEEE Transactions on Instrumentation and Measurement*, Vol. 67, No. 9, pp.2058–2068, https://doi.org/10.1109/TIM.2018.2813820.

Naha, A., Samanta, A.K., Routray, A. and Deb, A. (2016) 'A method for detecting half-broken rotor bar in lightly loaded induction motors using current', *IEEE Transactions on Instrumentation and Measurement*, Vol. 65, No. 7, pp.1614–1625, https://doi.org/10.1109/TIM.2016.2540941.

Nath, A.G., Sharma, A., Udmale, S.S. and Singh, S.K. (2020) 'An early classification approach for improving structural rotor fault diagnosis', *IEEE Transactions on Instrumentation and Measurement*, Vol. 70, pp.1–13, https://doi.org/10.1109/TIM.2020.3043959.

Nath, A.G., Udmale, S.S. and Singh, S. (2021) 'Role of artificial intelligence in rotor fault diagnosis: a comprehensive review', *Artificial Intelligence Review*, Vol. 54, pp.2609–2668, https://doi.org/10.1007/s10462-020-09910-w.

Nurrani, H., Nugroho, A.K. and Heranurweni, S. (2023) 'Image classification of vegetable quality using support vector machine based on convolutional neural network', *Jurnal RESTI (Rekayasa Sistem dan Teknologi Informasi)*, Vol. 7, No. 1, pp.168–178, https://doi.org/10.29207/resti.v7i1.4715.

Ordaz-Moreno, A., de Jesus Romero-Troncoso, R., Vite-Frias, J.A., Rivera-Gillen, J.R. and Garcia-Perez, A. (2008) 'Automatic online diagnosis algorithm for broken-bar detection on induction motors based on discrete wavelet transform for FPGA implementation', *IEEE Transactions on Industrial Electronics*, Vol. 55, No. 5, pp.2193–2202, https://doi.org/10.1109/TIE.2008.918613.

Palácios, R.H., da Silva, I.N., Godoy, W.F., Fabri, J.A. and de Souza, L.B. (2020) 'Voltage unbalance evaluation in the intelligent recognition of induction motor rotor faults', *Soft Computing*, Vol. 24, pp.16935–16946, https://doi.org/10.1007/s00500-020-04986-6.

Panagiotou, P.A., Arvanitakis, I., Lophitis, N., Antonino-Daviu, J.A. and Gyftakis, K.F. (2019a) 'A new approach for broken rotor bar detection in induction motors using frequency extraction in stray flux signals', *IEEE Transactions on Industry Applications*, Vol. 55, No. 4, pp.3501–3511, https://doi.org/10.1109/TIA.2019.2905803.

Panagiotou, P.A., Arvanitakis, I., Lophitis, N., Antonino-Daviu, J.A. and Gyftakis, K.F. (2019b) 'On the broken rotor bar diagnosis using time–frequency analysis: is one spectral representation enough for the characterisation of monitored signals?', *IET Electric Power Applications*, Vol. 13, No. 7, pp.932–942, https://doi.org/10.1049/iet-epa.2018.5512.

Patil, S., Jalan, A. and Marathe, A.M. (2022) 'Support vector machine for misalignment fault classification under different loading conditions using vibro-acoustic sensor data fusion', *Experimental Techniques*, Vol. 46, pp.957–971, https://doi.org/10.1007/s40799-021-00533-6.

Paul, I., Sahu, A., Das, P.K. and Meher, S. (2023) 'Deep convolutional neural network-based automatic detection of brain tumour', *2nd IEEE International Conference for Innovation in Technology (INOCON)*, pp.1–6, https://doi.org/10.1109/INOCON57975.2023.10101238.

Quiroz, J.C., Mariun, N., Mehrjou, M.R., Izadi, M., Misron, N. and Radzi, M.A. (2018) 'Fault detection of broken rotor bar in LS-PMSM using random forests', *Measurement*, Vol. 116, pp.273–280, https://doi.org/10.1016/j.measurement.2017.11.004.

Rangel-Magdaleno, J., Peregrina-Barreto, H., Ramirez-Cortes, J. and Cruz-Vega, I. (2017) 'Hilbert spectrum analysis of induction motors for the detection of incipient broken rotor bars', *Measurement*, Vol. 109, pp.247–255, https://doi.org/10.1016/j.measurement.2017.05.070.

Rodrigues, C.E., Júnior, C.L.N. and Rade, D.A. (2022) 'Application of machine learning techniques and spectrum images of vibration orbits for fault classification of rotating machines', *Journal of Control, Automation and Electrical Systems*, Vol. 33, No. 1, pp.333–344, https://doi.org/10.1007/s40313-021-00805-x.

Romero-Troncoso, R., Garcia-Perez, A., Morinigo-Sotelo, D., Duque-Perez, O., Osornio-Rios, R. and Ibarra-Manzano, M.A. (2016) 'Rotor unbalance and broken rotor bar detection in inverter-fed induction motors at start-up and steady-state regimes by high-resolution spectral analysis', *Electric Power Systems Research*, Vol. 133, pp.142–148, https://doi.org/10.1016/j.epsr.2015.12.009.

Sadeghian, A., Ye, Z. and Wu, B. (2009) 'Online detection of broken rotor bars in induction motors by wavelet packet decomposition and artificial neural networks', *IEEE Transactions on Instrumentation and Measurement*, Vol. 58, No. 7, pp.2253–2263, https://doi.org/10.1109/TIM.2009.2013743.

Sahu, A., Das, P.K. and Meher, S. (2023) 'High accuracy hybrid CNN classifiers for breast cancer detection using mammogram and ultrasound datasets', *Biomedical Signal Processing and Control*, Vol. 80, p.104292, https://doi.org/10.1016/j.bspc.2022.104292.

Sakallı, G. and Koyuncu, H. (2023) 'Identification of asynchronous motor and transformer situations in thermal images by utilizing transfer learning-based deep learning architectures', *Measurement*, Vol. 207, p.112380, https://doi.org/10.1016/j.measurement.2022.112380.

Siddiqui, K.M. and Giri, V. (2012) 'Broken rotor bar fault detection in induction motors using wavelet transform', *International Conference on Computing, Electronics and Electrical Technologies (ICCEET)*, pp.1–6, https://doi.org/10.1109/ICCEET.2012.6203753.

Singh, G. and Naikan, V.N.A. (2018) 'Detection of half broken rotor bar fault in VFD driven induction motor drive using motor square current MUSIC analysis', *Mechanical Systems and Signal Processing*, Vol. 110, pp.333–348, https://doi.org/10.1016/j.ymssp.2018.03.001.

Thakur, A.K., Kundu, P.K. and Das, A. (2021) 'Prediction of unknown fault of induction motor using SVM following decision-directed acyclic graph', *Journal of the Institution of Engineers (India): Series B*, Vol. 102, pp.573–583, https://doi.org/10.1007/s40031-021-00536-2.

Vas, P. (1993) *Parameter Estimation, Condition Monitoring, and Diagnosis of Electrical Machines*, Oxford University Press, Oxford, England.

Yaman, O. (2021) 'An automated faults classification method based on binary pattern and neighborhood component analysis using induction motor', *Measurement*, Vol. 168, p.108323, https://doi.org/10.1016/j.measurement.2020.108323.

Zolfaghari, S., Noor, S.B.M., M. Rezazadeh Mehrjou, Marhaban, M.H. and Mariun, N. (2017) 'Broken rotor bar fault detection and classification using wavelet packet signature analysis based on Fourier transform and multi-layer perceptron neural network', *Applied Sciences*, Vol. 8, No. 1, p.25, https://doi.org/10.3390/app8010025.